

Table 1
Primers utilized for PCR-based cloning and site-directed mutagenesis

The PCR product was cloned into a vector pSectTag/FRT/V5-His TOPO to express a fusion protein with a V5 tag or into a vector pcDNA4/HisMax-TOPO to express a fusion protein with a Xpress tag in HEK293 cells.

tion gradient of bovine serum albumin (BSA) (row 1; columns 3–8), four spots of a concentration gradient of a rabbit anti-GST antibody (row 1; columns 9–12), four spots of a concentration gradient of calmodulin (row 1; columns 13–16), 16 spots of a concentration gradient of GST (row 2; columns 1–16), two spots of buffer only (row 8; columns 9,10), and two spots of an anti- biotin antibody (row 8; columns 11,12). The complete list of 1752 target proteins immobilized on the microarray is shown in Supplementary Table 1 online.

Non-specific binding was blocked by incubating the microarray for 90 min in the PBST blocking buffer composed of 1% BSA and 0.1% Tween 20 in phosphate-buffered saline (PBS). Then, it was incubated for 30 min at 4 °C with the probe described above at a concentration of 50 µg/ml in the probing buffer composed of 1% BSA, 5 mM MgCl₂, 0.5 mM dithiothreitol (DTT), 0.05% Triton X-100, and 5% glycerol in PBS. The array was washed three times with the probing buffer, followed by incubation for 30 min at 4 °C with mouse monoclonal anti-V5 antibody conjugated with Alexa Fluor 647 (Invitrogen) at a concentration of 260 ng/ml in the probing buffer. The array was washed three times with the probing buffer, and then scanned by the GenePix 4200A scanner (Axon Instruments, Union City, CA) at a wavelength of 635 nm. The data were analyzed by using the ProtoArray Prospector software v2.0 (Invitrogen) following acquisition of the microarray lot-specific information online, including inter-lot variations in protein concentrations (<http://www.invitrogen.com/protoarray>). According to the default setting of the software, the spots showing the background-subtracted signal intensity value greater than the median plus three standard deviations of all the fluorescence intensities were considered as having a significant binding. The Z-score, an indicator for statistical evaluation of binding specificity, was calculated as the background-subtracted signal intensity value of the target protein minus the average of the background-subtracted signal intensity value from the negative control distribution, divided by the standard deviation of the negative control distribution. All the procedure described above could be accomplished within 5 h. The 14-3-3-binding consensus motif mode I (RSXpSXP) sequence located in target proteins was surveyed by the Scansite Motif Scanner, which assesses the probability of a site matching the candidate motif under high, medium, or low stringent conditions (Obenauer et al., 2003). The information on known 14-3-3 interactors was obtained from Biomolecular Interaction Network Database (BIND; <http://www.bind.ca>) and PubMed database search.

2.3. Transient expression of 14-3-3-binding proteins in HEK293 cells

To verify the results of microarray analysis, the ORF of the genes encoding EAP30 subunit of ELL complex (EAP30), dead box polypeptide 54 (DDX54), and src homology three (SH3) and cysteine rich domain (STAC) were amplified by PCR using Pfu-Turbo DNA polymerase and the primer sets listed in Table 1. They were then cloned into a mammalian expression vector pcDNA4/HisMax-TOPO (Invitrogen) to produce a fusion protein with an N-terminal Xpress tag. To express the STAC mutant



4

J.-i. Satoh et al. / Journal of Neuroscience Methods xxx (2005) xxx–xxx

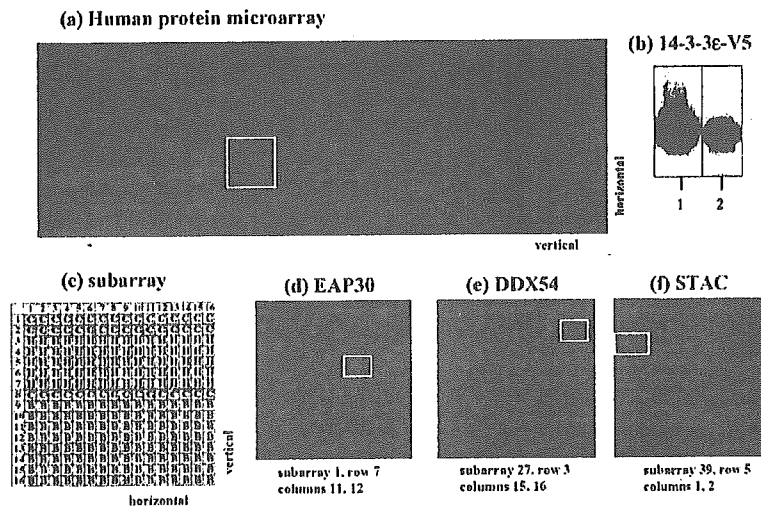


Fig. 1. Protein microarray analysis. (a) Human protein microarray. The microarray contains 1752 distinct human proteins of various functional classes spotted in duplicate on a nitrocellulose-coated glass slide. They are printed in an arrangement of 4×12 subarrays equally spaced in vertical and horizontal directions. A representative subarray is indicated by an enclosed yellow line. (b) Recombinant human 14-3-3 ϵ protein tagged with V5. One microgram of the protein was processed for Western blot analysis using anti-V5 antibody (lane 1) or anti-14-3-3 ϵ antibody (lane 2). (c) Layout of the subarray. Each subarray includes 16×16 spots composed of 48 control spots (C), 80 human proteins (H), and 128 blanks (B). The positive control spots include an Alexa Fluor 647-labeled antibody (rows 1, 8; columns 1, 2; strong signals), a concentration gradient of a biotinylated anti-mouse antibody with a capacity to bind to mouse monoclonal anti-V5 antibody conjugated with Alexa Fluor 647 (row 8; columns 3–8; signals visible on the higher concentration), and a concentration gradient of V5 protein (row 8; columns 13–16; signals visible on the higher concentration). (d) EAP30. (e) DDX54. (f) STAC. The three proteins indicated by an enclosed yellow line located on different subarrays (d, f) represent an example identified as showing significant binding to the probe.

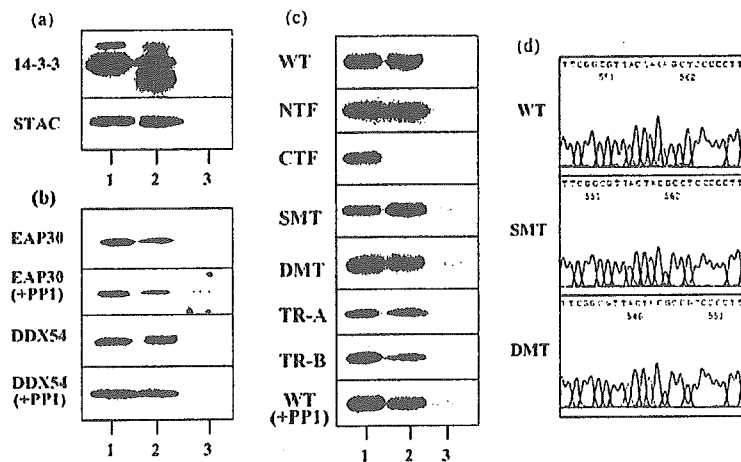


Fig. 2. Immunoprecipitation analysis of 14-3-3-binding proteins. (a) Binding of STAC to 14-3-3. Total protein extract of HEK293 cells expressing Xpress-tagged recombinant STAC was processed for immunoprecipitation (IP) with rabbit polyclonal antibody reacting with all 14-3-3 isoforms (K-19) or with normal rabbit IgG. The immunoprecipitates were then processed for Western blot analysis using mouse monoclonal antibody reacting with all 14-3-3 isoforms (H-8) (upper panel) or mouse monoclonal anti-Xpress antibody (lower panel). Lanes (1–3) represent (1) the input control, and IP with (2) K-19 and (3) normal rabbit IgG. (b) Binding of EAP30 and DDX54 to 14-3-3. Total protein of HEK293 cells expressing Xpress-tagged recombinant EAP30 or DDX54 extracted by using the lysis buffer with inclusion of phosphatase inhibitors or with inclusion of protein phosphatase-1 (PP1) instead of phosphatase inhibitors (+PP1) was processed for IP with K-19 or with normal rabbit IgG. The immunoprecipitates were then processed for Western blot analysis using anti-Xpress antibody. Lanes (1–3) represent (1) the input control, and IP with (2) K-19 and (3) normal rabbit IgG. (c) Binding of mutant and truncated STAC to 14-3-3. Total protein was extracted from HEK293 cells expressing a panel of Xpress-tagged recombinant STAC proteins. They include the full-length wild-type (WT) STAC, the N-terminal half (NTF), the C-terminal half (CTF), the S172A mutant (SMT), the S172A and S173A double mutant (DMT), the truncated form lacking the 14-3-3-binding consensus motif RYYSSP (TR-A), the truncated form lacking the cysteine-rich domain (CRD) (TR-B), and WT STAC isolated by using the lysis buffer with inclusion of PP1 instead of phosphatase inhibitors (WT + PP1). Primers utilized for PCR-based cloning and site-directed mutagenesis are listed in Table 1. The lysate was processed for IP with K-19 or with normal rabbit IgG. The immunoprecipitates were then processed for Western blot analysis using anti-Xpress antibody. Lanes (1–3) represent (1) the input control, and IP with (2) K-19 and (3) normal rabbit IgG. (d) The sequence of the 14-3-3-binding consensus motif located in amino acid residues 169–174 in expression vectors of STAC. The panels indicate WT (nucleotide sequence CGT-TAC-TAC-AGC-TCC-CCC: the corresponding amino acid sequence RYYSSP), SMT (CGT-TAC-TAC-GCC-TCC-CCC: RYYASP), and DMT (CGT-TAC-TAC-GCC-GCC-CCC: RYYAAP).

with a single amino acid substitution S172A (the single mutant; SMT) or with double amino acid substitutions S172A and S173A (the double mutant; DMT), the pcDNA4/HisMax-TOPO vector containing the wild-type (WT) STAC gene was modified by consecutive site-directed mutagenesis using QuikChange II site-directed mutagenesis kit (Stratagene) and the primer sets listed in Table 1. The mutations introduced in the vector were verified by sequencing analysis (Fig. 2d). All these vectors were transfected in HEK293 cells by Lipofectamine 2000 reagent.

2.4. Immunoprecipitation analysis

To prepare total protein extract, the cells were homogenized and incubated at room temperature for 30 min in M-PER lysis buffer (Pierce, Rockford, IL) supplemented with a cocktail of protease inhibitors (Sigma), with inclusion of phosphatase inhibitors (Sigma) to maintain the protein phosphorylation status or with inclusion of recombinant protein phosphatase-1 (PP1) catalytic subunit α -isoform (5 U/ml; Sigma) instead of phosphatase inhibitors to induce the protein dephosphorylation reaction (Ichimura et al., 2005), followed by centrifugation at 12,000 rpm at 4 °C for 20 min. After preclearance, the supernatant was incubated at 4 °C for 3 h with 30 μ g/ml rabbit polyclonal anti-14-3-3 protein antibody (K19)-conjugated agarose (Santa Cruz Biotechnology, Santa Cruz, CA) or the same amount of normal rabbit IgG-conjugated agarose (Santa Cruz Biotechnology). After several washes, the immunoprecipitates were processed for Western blot analysis using mouse monoclonal anti-14-3-3 protein antibody (H-8, Santa Cruz Biotechnology) and mouse monoclonal anti-Xpress antibody (Invitrogen). K-19 and H-8 antibodies recognize all 14-3-3 isoforms. The specific reaction was visualized using a chemiluminescent substrate (Pierce).

3. Results

3.1. Protein microarray analysis identified 20 distinct 14-3-3-binding partners

To analyze a high-density human protein microarray, the recombinant 14-3-3 ϵ protein tagged with V5 was purified from the supernatant of 293 eV5 cells secreting the recombinant protein in the culture medium. Western blot analysis verified the purity and specificity of the probe (Fig. 1b). Among 1752 proteins on the microarray, 20 were identified as the proteins showing significant binding to the probe (Table 2). All of these were previously unreported 14-3-3-binding partners by the BIND search. Seven were hypothetical clones of uncharacterized function, derived from the mammalian genome collection (MGC) or the full-length long Japan (FLJ). Thirteen annotated proteins included EAP30 subunit of ELL complex (EAP30) (Fig. 1d), lymphocyte cytosolic protein 2 (LCP2), methionine aminopeptidase 2 (METAP2), melanoma antigen family B, 4 (MAGEB4), chondroitin 4 sulfotransferase 11 (CHST11), nuclear interacting partner of anaplastic lymphoma kinase (ZC3HC1), minichromosome maintenance deficient 10 (MCM10), DEAD box polypeptide 54 (DDX54) (Fig. 1e), heterogeneous nuclear ribonucleo-

protein C (HNPRC), fibroblast growth factor 12 (FGF12), glutathione S-transferase M3 (GSTM3), src homology three (SH3) and cysteine rich domain (STAC) (Fig. 1f), and ATPase, H⁺ transporting, lysosomal, 21 kDa, V0 subunit C'' (ATP6V0B). The 14-3-3-binding consensus motif mode I (RSX_pSXP) was found only in STAC (*pS172*) and HNRPC (*pS125*) by the ScanSite Motif Scanner search under the high stringent condition, while 15 of 20 proteins have one or several motifs when a query with the medium or low stringency was performed (Table 2).

3.2. Immunoprecipitation analysis validated the specific binding to 14-3-3

EAP30, DDX54, and STAC were selected to verify the results of microarray analysis, in view of their higher Z-scores. The recombinant proteins were expressed in HEK293 cells, which constitutively express a substantial amount of endogenous 14-3-3 protein. Total protein was extracted by using the lysis buffer with inclusion of phosphatase inhibitors to maintain the protein phosphorylation status or with inclusion of recombinant protein phosphatase-1 (PP1) instead of phosphatase inhibitors to induce the protein dephosphorylation reaction, followed by processing for immunoprecipitation (IP) with rabbit polyclonal antibody reacting with all 14-3-3 isoforms (K-19) or with normal rabbit IgG. K19 coimmunoprecipitated 14-3-3 and STAC from the lysate of HEK293 cells expressing the recombinant STAC protein, whereas normal rabbit IgG did not pull down these proteins (Fig. 2a). K-19 immunoprecipitated EAP30 and DDX54 from the lysate of HEK293 cells expressing the recombinant EAP30 or DDX54 protein, respectively, under both phosphorylated and dephosphorylated conditions (Fig. 2b). These results indicate that EAP30, DDX54, and STAC could interact with the endogenous 14-3-3 protein in HEK293 cells where the corresponding recombinant proteins were expressed.

STAC has the highly stringent 14-3-3-binding consensus motif RYYSSP in amino acid residues 169–174 (*pS172*), as suggested by the ScanSite Motif Scanner (Table 2). Therefore, a possible involvement of this motif in binding to 14-3-3 was investigated by IP analysis of a series of mutant and truncated STAC proteins (Table 1). K-19 immunoprecipitated the full-length wild-type (WT) STAC comprised of amino acid residues 2–402 (Fig. 2a and c). K-19 also pulled down the S172A mutant (SMT), and the S172A and S173A double mutant (DMT), and the N-terminal half (NTF; amino acid residues 2–233) from the lysate of HEK293 cells expressing the corresponding recombinant proteins (Fig. 2c). In contrast, K-19 did not pull down the C-terminal half (CTF; amino acid residues 234–402) (Fig. 2c). These observations indicate that the RYYSSP motif is not essential for binding of STAC to 14-3-3. This was confirmed by the observations that K-19 immunoprecipitated the truncated form lacking the RYYSSP sequence (TR-A; amino acid residues 2–164) and the shortest form lacking both the RYYSSP sequence and the cysteine-rich domain (CRD) (TR-B; amino acid residues 2–105) from the lysate of HEK293 cells expressing the corresponding recombinant proteins (Fig. 2c). Finally, the full-length WT STAC interacted with 14-3-3 under the dephosphorylated condition (Fig. 2c). These observations indicate that the 14-

Table 2
Twenty 14-3-3-binding proteins identified by protein microarray analysis

No.	Symbol	Database ID	Protein name	Predictive biological function	14-3-3-binding consensus motif mode I	Stringency level of the binding motif	Subarray	Row	Column	Z-score
1	EAP30	NM_007241	EAP30 subunit of ELL complex	a 30-kDa component of the ELL complex that confers derepression of transcription by RNA polymerase II	· No sites	NA	1	7	11	22.8593
2	FLJ10415	NM_018089	Hypothetical protein, cDNA clone MGC:969	Unknown	S258: ARGGPSH <u>SAGANLRR</u>	Low	5	4	11	24.60829
3	LOC57228	NM_020467	Hypothetical protein	Unknown	S405: SPKQGSG <u>SEGEDGFQ</u> S525: PADPRV <u>L</u> LLSAPLG S690: VNTRRCW <u>S</u> CGASLQG	Low Low Low	·	12	4.16265	
4	MGC17403	NM_152634	Hypothetical protein	Unknown	T274: KQLRASYT <u>ESCIQE</u> H	Low	11	3	1	4.35203
5	LCP2	NM_005565	Lymphocyte cytosolic protein 2	A 72-kDa protein (SLP76) that associates with the Grb2 adaptor protein, provides a substrate of the ZAP-70 protein tyrosine kinase, and plays a role in promoting T cell development and activation	S297: TTER <u>HERS</u> SPLP <u>GKK</u>	Low	13	5	11	16.84741
6	METAP2	NM_006838	Methionine aminopeptidase 2	A 67-kDa protein that interacts with eukaryotic initiation factor-2 (eIF-2) and regulates protein synthesis	S376: SSETPOS <u>ASLPPPTFSQ</u> T456: DSSKKIT <u>TNPYVLMV</u>	Low Low	12	6	11	17.1519
7	MAGEB4	NM_002367	Melanoma antigen family B, 4	A member of the MAGEB family expressed in testis whose function remains unknown	T113: KRGPKV <u>QTDP</u> PSVPI S152: TAAWR <u>TTSEEKK</u> KALD T18: AREKR <u>QRTRGQ</u> TQDL	Low Medium	15	6	11	4.04754
8	CHST11	NM_018413	Chondroitin 4-sulfotransferase 11	A member of HNK-1ST family GalNAc 4-O-sulfotransferase that plays a role in chondroitin sulfate and dermatan sulfate biosynthesis	T194: GNQSSAW <u>T</u> PRNGLL S339: SAYSRAT <u>SSSSQQPM</u>	Low Low	18	3	7	4.08838
9	ZC3HC1	NM_016478	Nuclear interacting partner of anaplastic lymphoma kinase (ALK)	No sites	S93: TDTCR <u>ANSAT</u> SRKRR	Medium	20	5	3	4.35366
					S56: DICCR <u>KGSRS</u> PLQEL S194: EPF <u>ERLYVSAYRNKF</u> T	Low Low		4	3.92871	
					NA		23	3	3	3.33458
								4		

J.-i. Satoh et al. / Journal of Neuroscience Methods xxx (2005) xxx–xxx

Model	Gene ID	Protein Name	Function	Sequence	Scoring	Score	Length	Accession
10	MCM10	NM_018518	Minichromosome maintenance deficient 10	A key component of the pre-replication complex (pre-RC) that is essential for the initiation of DNA replication	S90: AQPRTGSEPPRLEG	Medium	25	3 13 4.26291
11	DDX54	NM_024072	DEAD (Asp-Glu-Ala-Asp) box polypeptide 54	A 97-kDa RNA helicase (DP97) that interacts with estrogen receptor (ER) and represses the transcription of ER-regulated genes	S35: KPAIKSISASALLKQ S55: LEMRRRKSEEEIQKRF S302: PCGNRSISLDRLPNK T329: DGMLKEKIGPKIGGE T95: EDKKKIKTESGRYIS	Low Low Low Low Low	14	4.12552
12	HNPRC	NM_004500	Heterogeneous nuclear ribonucleoprotein C	A member of heterogeneous nuclear ribonucleoproteins (hnRNPs) involved in pre-mRNA processing, mRNA metabolism and transport	S102: TESGRYI <u>S</u> SYKRDL S125: DYTYDRMYS <u>S</u> TARVPP	Low High	28	16 4.81248
13	LOC137781	BC032347	Hypothetical gene, cDNA clone MGC:40429	Unknown	S158: NTSSRGK <u>S</u> GFNKSKG S170: KSGORGSKSGKLKG S240: ETNVKME <u>S</u> EGGADDSS No sites	Low Low Low NA	10	5.18382
14	LOC92345	NM_138386	Hypothetical protein	Unknown	S339: QGRKKLK <u>S</u> FFNEPGE T344: GYNRREF <u>R</u> GFCSRAR S467: PLINLPP <u>S</u> LPPPPP S150: VCMYREQ <u>S</u> LEIGEK	Low Low Low Low	32	5 13 3.55366
15	FGF12	NM_004113	Fibroblast growth factor 12, transcript variant 2	A member of the FGF family that plays a role in nervous system development and function	S165: QGRSRK <u>S</u> SGPTTMNG S64: GIKLRSFSV	Low Low	34	6 5 3.73933
16	GSTM3	NM_000849	Glutathione S-transferase M3 (brain)	A cytoplasmic glutathione S-transferase of the mu class that plays a role in detoxification of carcinogens, therapeutic drugs, environmental toxins, and products of oxidative stress	S66: TKSLRS <u>K</u> SADNNFQR S255: DLRKRSNSVFTYPEN S46: QKLKRS <u>I</u> SEFKTKSLR S51: SLSFKTK <u>S</u> LRSKSAD S66: NFFQRTN <u>S</u> EDMKLQA S233: GYDLRKRS <u>N</u> SVFTYP	Medium Medium Low Low Low Low	38	5 15 7.82029
17	STAC	NM_003149	src homology three (SH3) and cysteine rich domain	A 47-kDa protein with a SH3 and a cysteine-rich domain that plays a role in the neuron-specific signal transduction pathway	S172: KGFRRY <u>S</u> SPLLIHE	High	39	5 1 7.70889

Table 2 (Continued)

No.	Symbol	Database ID	Protein name	Putative biological function	14-3-3-binding consensus motif mode I	Stringency level of the binding motif	Subarray	Row	Column	Z-score
18	FLJ10156	NM_019013	Hypothetical protein, cDNA clone MGC:961	Unknown	S16: GTSYVRRRS <u>L</u> QHQEQL	Low	41	3	7	7.31156
19	ATP6V0B	NM_004047	ATPase, H ⁺ transporting, lysosomal, 21 kD, V0 subunit C"	A 23-kDa component of vacuolar ATPase that mediates acidification of intracellular organelles	T190: FRSPYSS <u>T</u> EPLCSPS	Low	NA	43	7	3
20	FLJ25758	NM_001011541	Hypothetical protein, clone MGC:33355	Unknown	No sites	No sites	NA	48	7	4.18864

Among 1752 proteins on the microarray, 20 were identified as showing a significant interaction, based on the signal intensity value exceeding the median plus three standard deviations of all the fluorescence intensities by analyzing with ProtoArray Prospector software. They are listed with the 14-3-3-binding consensus motif (putative phosphoserine and phosphothreonine indicated by underline) and its stringency level by the ScanSite Motif Scanner, the position on the array, and the Z-score calculated as described in Section 2. Abbreviations: FLJ, the full-length long Japan; MCG, mammalian gene collection; NA, not available.

3-3-interacting domain is located in the N-terminal segment spanning amino acid residues 2–105 of STAC, and the interaction is independent of serine/threonine-phosphorylation of the binding domain of STAC.

4. Discussion

The present study was designed to rapidly and systematically identify 14-3-3-binding proteins by analyzing a high-density protein microarray. The array included 1752 proteins derived from multiple gene families of biological importance, including cell-signaling proteins, kinases, membrane-associated proteins, and metabolic proteins. In general, protein microarray has its own limitations associated with the expression and purification of a wide variety of target proteins. In the microarray we utilized, the target proteins were expressed in a baculovirus expression system, purified under native conditions, and spotted on the slides to ensure the preservation of native structure, posttranslational modifications, including glycosylation and serine phosphorylation (Culleré et al., 1998; Tennagels et al., 1999), and proper functionality. Immunolabeling of the array with anti-phosphotyrosine (pTyr) antibody indicated that approximately 10–20% of the proteins on the array are phosphorylated (the unpublished data of Invitrogen Technical Service). When this microarray was utilized for kinase substrate identification, most of known kinases immobilized on the array are enzymatically active with the capacity of some degree of autophosphorylation, suggesting that they are certainly phosphorylated on tyrosine, serine, and threonine residues (see the Protoarray application note on <http://www.invitrogen.com/protoarray>). However, we could not currently validate the precise levels of phosphorylation of individual proteins, because of a lack of anti-phosphoserine (pSer) and anti-phosphothreonine (pThr) antibodies suitable for detection of pSer and pThr residues of the proteins on glass slide.

The protein microarray utilized in the present study includes 11 known 14-3-3-binding proteins, such as PCTAIRE protein kinase 1 (PCTK1) (Graeser et al., 2002), protein kinase C zeta (PRKCZ) (van der Hoeven et al., 2000), keratin 18 (KRT18) (Ku et al., 1998), myosin light polypeptide kinase (MYLK) (Haydon et al., 2002), v-abl Abelson murine leukemia viral oncogene homolog 1 (ABL1) (Yoshida et al., 2005), v-akt murine thymoma viral oncogene homolog 1 (AKT1) (Powell et al., 2002), epidermal growth factor receptor (EGFR) (Oksvold et al., 2004), cell division cycle 2 (CDC2) (Chan et al., 1999), mitogen-activated protein kinase kinase kinase 1 (MAP3K1) (Fanger et al., 1998), mitogen-activated protein kinase-activated protein kinase 2 (MAPKAPK2) (Powell et al., 2003), and stratifin (SFN) (Benzinger et al., 2005) (Table 3). All of these were not identified as a 14-3-3-binding protein in the present study. Therefore, the possibility could not be excluded that some 14-3-3 binding partners were not detected due to imperfect phosphorylation of the proteins on the array or due to 14-3-3 isoform-specific binding. Calmodulin, another known 14-3-3 interactor (Luk et al., 1999), was included as a negative control on the array and identified as negative in the present study, because the calcium-dependent interaction between 14-3-3 and calmodulin could not be detected under the calcium-free conditions we employed.

Table 3

Eleven known 14-3-3-binding proteins immobilized on the protein microarray utilized in the present study

Gene name	Database ID	Reference
PCTAIRE protein kinase 1 (PCTK1), transcript variant 3	NM_033019	Graeser et al. (2002)
Protein kinase C, zeta (PRKCZ)	NM_002744	van der Hoeven et al. (2000)
Keratin 18 (KRT18), transcript variant 1	NM_000224	Ku et al. (1998)
Myosin, light polypeptide kinase (MYLK), transcript variant 6	NM_005965	Haydon et al. (2002)
V-abl Abelson murine leukemia viral oncogene homolog 1 (ABL1), transcript variant a	NM_005157	Yoshida et al. (2005)
V-akt murine thymoma viral oncogene homolog 1 (AKT1), transcript variant 1	NM_005163	Powell et al. (2002)
Epidermal growth factor receptor (EGFR), transcript variant 1	NM_005228	Oksvold et al. (2004)
Cell division cycle 2 (CDC2), transcript variant 1	NM_001786	Chan et al. (1999)
Mitogen-activated protein kinase kinase kinase 1 (MAP3K1)	XM_042066	Fanger et al. (1998)
Mitogen-activated protein kinase-activated protein kinase 2 (MAPKAPK2), transcript variant 1	NM_004759	Powell et al. (2003)
14-3-3 Sigma, stratifin (SFN)	NM_006142	Benzinger et al. (2005)

The known 14-3-3-binding proteins, which were spotted on the protein microarray but were not detected in the present study are listed. The 14-3-3-binding proteins validated by definitive evidence are selected and shown with references.

Increasing studies indicate that 14-3-3-binding phosphorylation sites do not exactly fit the consensus motif (Aitken et al., 2002; Ku et al., 1998) and a second site is required to enhance a stable 14-3-3-target interaction (MacKintosh, 2004), and show that the 14-3-3 protein interacts with a set of target proteins in a phosphorylation-independent manner (Dai and Murakami, 2003; Henriksson et al., 2002; Zhai et al., 2001). Supporting the latter possibility, the present observations showed that the interaction of 14-3-3 with target proteins is independent of serine/threonine-phosphorylation of the binding sites of EAP30, DDX54, and STAC. This suggests that substantial numbers of 14-3-3 binding partners identified by protein microarray analysis, if not all, employ phosphorylation-independent binding domains.

All the procedure required for microarray analysis takes approximately 5 h. This analysis identified a set of 20 human proteins as 14-3-3 interactors, most of which were previously unreported except for glutathione S-transferase M3 (GSTM3) that was found as one of binding partners by 14-3-3 affinity purification of HeLa cell protein extracts (Pozuelo Rubio et al., 2004). Unexpectedly, the highly stringent 14-3-3-binding consensus motif was identified only in two, such as STAC and HNPRC, by the Scansite Motif Scanner search, while 15 of 20 proteins have one or several motifs when a query with the medium or low stringency was performed (Table 2). The specific binding to 14-3-3 of EAP30, DDX54, and STAC was verified by immunoprecipitation analysis of the recombinant proteins expressed in HEK293 cells. These results indicate that protein microarray is a powerful tool for rapid identification of protein–protein interactions, including those unpredicted by the Database search.

Among the 14-3-3-binding partners we identified, several proteins could be categorized as a component of multimolecular complexes involved in transcriptional regulation. ELL is a human oncogene encoding a RNA polymerase II (Pol II) transcription factor that promotes transcription elongation (Schmidt et al., 1999). EAP30 is a 30-kDa component of the ELL complex where EAP30 confers derepression of transcription by Pol II (Schmidt et al., 1999). A recent study showed that EAP30 could interact with the tumor susceptibility gene TSG101 product, a cellular factor that plays a key role in packaging of HIV

virions (von Schwedler et al., 2003). DDX54 is a 97-kDa RNA helicase (DP97) that interacts with estrogen receptor (ER) and represses the transcription of ER-regulated genes (Rajendran et al., 2003). A recent study by using chromatin immunoprecipitation (ChIP) assay combined with promoter microarray analysis showed that hepatocyte nuclear factor 4-alpha (HNF4α), a master regulator of hepatocyte gene expression, interacts with the DDX54 gene promoter, together with Pol II (Odom et al., 2004). HNPRC is a member of heterogeneous nuclear ribonucleoproteins (hnRNPs) involved in pre-mRNA processing, mRNA metabolism and transport (Nakagawa et al., 1986). Increasing evidence indicates that the 14-3-3 protein and its targets are widely distributed in various subcellular compartments, including the nucleus (Dougherty and Morrison, 2004; Meek et al., 2004).

STAC is a 47-kDa cytosolic protein that has a cysteine-rich domain (CRD) of the protein kinase C family in the N-terminal half (NTF), and a src homology three (SH3) domain in the C-terminal half (CTF), suggesting its function as an adapter on which divergent signaling pathways converge (Hardy et al., 2005; Suzuki et al., 1996). STAC is expressed predominantly in the brain with the distribution in a defined population of neurons (Suzuki et al., 1996). IP analysis of mutant and truncated forms argued against an active involvement of the most stringent motif RYYSSP (*pS172*) of STAC in its binding to 14-3-3. The present observations indicated that the 14-3-3-interacting domain is located in the N-terminal segment spanning amino acid residues 2–105 of STAC and the interaction is serine/threonine phosphorylation-independent.

In conclusion, protein microarray is a useful tool for rapid and comprehensive profiling of 14-3-3-binding proteins, although the validation of the results by different methods is highly important.

Acknowledgements

This work was supported by grants from Research on Psychiatric and Neurological Diseases and Mental Health, the Ministry of Health, Labour and Welfare of Japan (H17-020), Research on Health Sciences Focusing on Drug Innovation, the Japan Health Sciences Foundation (KH21101), the Grant-in-Aid for Scienc-

443 tific Research, the Ministry of Education, Science, Sports and
 444 Culture (B2-15390280 and PA007-16017320), and the Program
 445 for Promotion of Fundamental Studies in Health Sciences of the
 446 National Institute of Biomedical Innovation (NIBIO), Japan.

447 Appendix A. Supplementary data

448 Supplementary data associated with this article can be found,
 449 in the online version, at 10.1016/j.jneumeth.2005.09.015.

450 References

- Aitken A, Baxter H, Dubois T, Clokie S, Mackie S, Mitchell K, Peden A, Zemlickova E. 14-3-3 proteins in cell regulation. *Biochem Soc Trans* 2002;30:351–60.
- Benzinger A, Muster N, Koch HB, Yates 3rd JR, Hermeking H. Targeted proteomic analysis of 14-3-3 sigma, a p53 effector commonly silenced in cancer. *Mol Cell Proteomics* 2005;4:785–95.
- Berg D, Holzmann C, Riess O. 14-3-3 proteins in the nervous system. *Nat Rev Neurosci* 2002;4:752–62.
- Chan SM, Ermann J, Su L, Fathman CG, Utz PJ. Protein microarrays for multiplex analysis of signal transduction pathways. *Nat Med* 2004;10:1390–6.
- Chan TA, Hermeking H, Lengauer C, Kinzler KW, Vogelstein B. 14-3-3 σ is required to prevent mitotic catastrophe after DNA damage. *Nature* 1999;401:616–20.
- Chen H-K, Fernandez-Funez P, Acevedo SF, Lam YC, Kaytor MD, Fernandez MH, Aitken A, Skoulakis EM, Orr HT, Botas J, Zoghbi HY. Interaction of Akt-phosphorylated ataxin-1 with 14-3-3 mediates neurodegeneration in spinocerebellar atrophy type 1. *Cell* 2003;113:457–68.
- Culleré X, Rose P, Thathamangalam U, Chatterjee A, Mullane KP, Pallas DC, Benjamin TL, Roberts TM, Schaffhausen BS. Serine 257 phosphorylation regulates association of polyomavirus middle T antigen with 14-3-3 proteins. *J Virol* 1998;72:558–63.
- Dai J-G, Murakami K. Constitutively and autonomously active protein kinase C associated with 14-3-3 ζ in the rodent brain. *J Neurochem* 2003;84:23–34.
- Dougherty MK, Morrison DK. Unlocking the code of 14-3-3. *J Cell Sci* 2004;117:1875–84.
- Fanger GR, Widmann C, Porter AC, Sather S, Johnson GL, Vaillancourt RR. 14-3-3 proteins interact with specific MEK kinases. *J Biol Chem* 1998;273:3476–83.
- Fu H, Subramanian RR, Masters SC. 14-3-3 proteins: structure, function, and regulation. *Annu Rev Pharmacol Toxicol* 2000;40:617–47.
- Graeser R, Gannon J, Poon RYC, Dubois T, Aitken A, Hunt T. Regulation of the CDK-related protein kinase PCTAIRE-1 and its possible role in neurite outgrowth in Neuro-2A cells. *J Cell Sci* 2002;115:3479–90.
- Hardy K, Mansfield L, Mackay A, Benvenuti S, Ismail S, Arora P, O'Hare MJ, Jat PS. Transcriptional networks and cellular senescence in human mammary fibroblasts. *Mol Biol Cell* 2005;16:943–53.
- Haydon CE, Watt PW, Morrice N, Knebel A, Gaestel M, Cohen P. Identification of a phosphorylation site on skeletal muscle myosin light chain kinase that becomes phosphorylated during muscle contraction. *Arch Biochem Biophys* 2002;397:224–31.
- Henriksson ML, Francis MS, Peden A, Aili M, Stefansson K, Palmer R, Aitken A, Hallberg B. A nonphosphorylated 14-3-3 binding motif on exoenzyme S that is functional in vivo. *Eur J Biochem* 2002;269:4921–9.
- Ichimura T, Yamamura H, Sasamoto K, Tominaga Y, Taoka M, Kakiuchi K, Shinkawa T, Takahashi N, Shimada S, Isobe T. 14-3-3 proteins modulate the expression of epithelial Na⁺ channels by phosphorylation-dependent interaction with Nedd4-2 ubiquitin ligase. *J Biol Chem* 2005;280:13187–94.
- Jin J, Smith FD, Stark C, Wells CD, Fawcett JP, Kulkarni S, Metalnikov P, O'Donnell P, Taylor P, Taylor L, Zouman A, Woodgett JR, Langeberg LK, Scott JD, Pawson T. Proteomic, functional, and domain-based analysis of in vivo 14-3-3 binding proteins involved in cytoskeletal regulation and cellular organization. *Curr Biol* 2004;14:1436–50.
- Kawamoto Y, Akiguchi I, Nakamura S, Honjyo Y, Shibasaki H, Budka H. 14-3-3 proteins in Lewy bodies in Parkinson disease and diffuse Lewy body disease brains. *J Neuropathol Exp Neurol* 2002;61:245–53.
- Ku N-O, Liao J, Omary MB. Phosphorylation of human keratin 18 serine 33 regulates binding to 14-3-3 proteins. *EMBO J* 1998;17:1892–906.
- Layfield R, Fergusson J, Aitken A, Lowe J, Landon M, Mayer RJ. Neurofibrillary tangles of Alzheimer's disease brains contain 14-3-3 proteins. *Neurosci Lett* 1996;209:57–60.
- Luk SCW, Ngai S-M, Tsui SKW, Fung K-P, Lee C-Y, Waye MMY. In vivo and in vitro association of 14-3-3 epsilon isoform with calmodulin: implication for signal transduction and cell proliferation. *J Cell Biochem* 1999;73:31–5.
- MacBeath G, Schreiber SL. Printing proteins as microarrays for high-throughput function determination. *Science* 2000;289:1760–3.
- MacKintosh C. Dynamic interactions between 14-3-3 proteins and phosphoproteins regulate diverse cellular processes. *Biochem J* 2004;318:329–42.
- Malaspina A, Kaushik N, de Belleroche J. A 14-3-3 mRNA is up-regulated in amyotrophic lateral sclerosis spinal cord. *J Neurochem* 2000;75:2511–20.
- Meek SEM, Lane WS, Piwnica-Worms H. Comprehensive proteomic analysis of interphase and mitotic 14-3-3-binding proteins. *J Biol Chem* 2004;279:32046–54.
- Michaud GA, Salcius M, Zhou F, Bangham R, Bonin J, Guo H, Snyder M, Predki PF, Schweitzer BI. Analyzing antibody specificity with whole proteome microarrays. *Nat Biotechnol* 2003;21:1509–12.
- Nakagawa TY, Swanson MS, Wold BJ, Dreyfuss G. Molecular cloning of cDNA for the nuclear ribonucleoprotein particle C proteins: a conserved gene family. *Proc Natl Acad Sci USA* 1986;83:2007–11.
- Obenauer JC, Cantley LC, Yaffe MB. Scansite 2.0: Proteome-wide prediction of cell signaling interactions using short sequence motifs. *Nucl Acids Res* 2003;31:3635–41.
- Odom DT, Zizlsperger N, Gordon DB, Bell GW, Rinaldi NJ, Murray HL, Volkeri TL, Schreiber J, Rolfe PA, Gifford DK, Fraenkel E, Bell GI, Young RA. Control of pancreas and liver gene expression by HNF transcription factors. *Science* 2004;303:1378–81.
- Oksvold MP, Huitfeld HS, Langdon WY. Identification of 14-3-3 ζ as an EGF receptor interacting protein. *FEBS Lett* 2004;569:207–10.
- Pozuelo Rubio M, Geraghty KM, Wong BH, Wood NT, Campbell DG, Morrice N, Mackintosh C. 14-3-3-affinity purification of over 200 human phosphoproteins reveals new links to regulation of cellular metabolism, proliferation and trafficking. *Biochem J* 2004;379:395–408.
- Powell DW, Rane MJ, Chen Q, Singh S, McLeish KR. Identification of 14-3-3 ζ as a protein kinase B/Akt substrate. *J Biol Chem* 2002;277:21639–42.
- Powell DW, Rane MJ, Joughin BA, Kalmukova R, Hong J-H, Tidor B, Dean WL, Pierce WM, Klein JB, Yaffe MB, McLeish KR. Proteomic identification of 14-3-3 ζ as a mitogen-activated protein kinase-activated protein kinase 2 substrate: role in dimer formation and ligand binding. *Mol Cell Biol* 2003;23:5376–87.
- Rajendran RR, Nye AC, Frasor J, Balsara RD, Martini PG, Katzenellenbogen BS. Regulation of nuclear receptor transcriptional activity by a novel DEAD box RNA helicase (DP97). *J Biol Chem* 2003;278:4628–38.
- Satoh J, Kuroda Y. Differential gene expression between human neurons and neuronal progenitor cells in culture: an analysis of arrayed cDNA clones in NTera2 human embryonal carcinoma cell line as a model system. *J Neurosci Meth* 2000;94:155–64.
- Satoh J, Yamamura T. Gene expression profile following stable expression of the cellular prion protein. *Cell Mol Neurobiol* 2004;24:793–814.
- Satoh J, Yamamura T, Arima K. The 14-3-3 protein ϵ isoform expressed in reactive astrocytes in demyelinating lesions of multiple sclerosis binds to vimentin and glial fibrillary acidic protein in cultured human astrocytes. *Am J Pathol* 2004;165:577–92.
- Schmidt AE, Miller T, Schmidt SL, Shiekhattar R, Shilatifard A. Cloning and characterization of the EAP30 subunit of the ELL complex that confers derepression of transcription by RNA polymerase II. *J Biol Chem* 1999;274:21981–5.
- Suzuki H, Kawai J, Taga C, Yaoi T, Hara A, Hirose K, Hayashizaki Y, Watanabe S. Stac, a novel neuron-specific protein with cysteine-rich and SH3 domains. *Biochem Biophys Res Commun* 1996;229:902–9.

- 573 Tennagels N, Hube-Magg C, Wirth A, Noelle V, Klein HW. Expression, 590
574 purification, and characterization of the cytoplasmic domain of the human 591
575 IGF-1 receptor using a baculovirus expression system. *Biochem Biophys 592*
576 *Res Commun* 1999;260:724–8. 593
577 van der Hoeven PCJ, van der Wal JCM, Ruurs P, van Blitterswijk WJ. Protein 594
578 kinase C activation by acidic proteins including 14-3-3. *Biochem J 595*
579 2000;347:781–5. 596
580 van Hemert MJ, Steensma HY, van Heusden GPH. 14-3-3 proteins: key 597
581 regulators of cell division, signaling and apoptosis. *Bioessays 598* 2001;23:936–47.
582 Vidalain PO, Boxem M, Ge H, Li S, Vidal M. Increasing specificity in high- 599
583 throughput yeast two-hybrid experiments. *Methods 600* 2004;32:363–70.
584 von Mering C, Krause R, Snel B, Cornell M, Oliver SG, Fields S, Bork P. 601
585 Comparative assessment of large-scale data sets of protein-protein 602 interactions. *Nature 603* 2002;417:399–403.
586 von Schwedler UK, Stuchell M, Müller B, Ward DM, Chung HY, Morita E, 604
587 Wang HE, Davis T, He GP, Cimbara DM, Scott A, Kräusslich HG, Kaplan 605
588 J, Morham SG, Sundquist WI. The protein network of HIV budding. *Cell 606*
589 2003;114:701–13. 607
- Yoshida K, Yamaguchi T, Natsume T, Kufe D, Miki Y. JNK phosphorylation of 14-3-3 proteins regulates nuclear targeting of c-Abl in the apoptotic response to DNA damage. *Nat Cell Biol 2005;7:278–85.*
- Zerr I, Bodemer M, Gefeller O, Otto M, Poser S, Wiltfang J, Windl O, Kreitzschmar HA, Weber T. Detection of 14-3-3 protein in the cerebrospinal fluid supports the diagnosis of Creutzfeldt–Jakob disease. *Ann Neurol 1998;43:32–40.*
- Zhai J, Lin H, Shamim M, Schlaepfer WW, Cañete-Soler R. Identification of a novel interaction of 14-3-3 with p190RhoGEF. *J Biol Chem 2001;276:41318–24.*
- Zhang LV, Wong SL, King OD, Roth FP. Predicting co-complexed protein pairs using genomic and proteomic data integration. *BMC Bioinformat 2004;5:38–52.*
- Zhu H, Bilgin M, Bangham R, Hall D, Casamayor A, Bertone P, Lan N, Jansen R, Bidlingmaier S, Houfek T, Mitchell T, Miller P, Dean RA, Gerstein M, Snyder M. Global analysis of protein activities using proteome chips. *Science 2001;293:2101–5.*

DNA マイクロアレイによる多発性硬化症の免疫病態の解析

佐藤 準一

日本神経免疫学会機関誌 神経免疫学 Vol.13 No.2

2005

<特集 | サイトカイン・ケモカインからみた多発性硬化症の病型と病態>

DNAマイクロアレイによる多発性硬化症の免疫病態の解析

佐藤 準一^{1,2)}

DNA Microarray Analysis Clarifies Immunopathogenesis of Multiple Sclerosis

Jun-ichi Satoh^{1,2)}**Abstract**

Multiple sclerosis (MS) is an inflammatory demyelinating disease of the central nervous system (CNS) white matter mediated by an autoimmune process whose development is triggered by a complex interplay of both genetic and environmental factors. MS shows a great range of phenotypic variability in terms of the disease course, lesion distribution, therapeutic response to IFN β , and pathological aspects, suggesting that MS is a kind of neurological syndrome caused by different immunopathological mechanisms leading to the final common pathway that provokes inflammatory demyelination. DNA microarray technology is a novel approach to systematically monitoring the expression of a large number of genes. It gives us new insights into the complexity of molecular interactions promoting the autoimmune process in MS. By microarray analysis followed by hierarchical clustering analysis, we found that T cell gene expression profiling is valuable to identify distinct subgroups of MS associated with differential disease activity and therapeutic response to IFN β . These observations suggest that microarray analysis is highly valuable for designing personalized treatment for heterogeneous populations of MS.

Key words : DNA microarray, gene expression profile, multiple sclerosis, personalized medicine

はじめに

多発性硬化症 (multiple sclerosis; MS) は中枢神経系白質に炎症性脱髓鞘が多発し、様々な神経症状が再発を繰り返して進行する難病である。MS 発症機序は十分解明されていないが、多数の遺伝的要因と環境因子の存在下で、脳炎惹起性髓鞘抗原に分子相同性を示すウイルスなどの外来抗原を認識し活性化した自己反応性 CD4 $^+$ Th1 T 細胞が、血液脳関門を通過して中枢神経系組織内に浸潤し、マクロファージ・ミクログリアを活性化して TNF α などの炎症増強因子の産生を誘導し、脱髓が惹起されると考えられている（自己免疫機序）¹⁾。回復期には髓鞘再生を認めるが、炎症が高度で遷延化すると髓鞘再生不全・軸索傷害・神経変性を來して不可逆的な機能障害を残す。

近年欧米・本邦で実施された大規模臨床試験により、インターフェロンベータ (interferon-beta; IFN β) の MS 再発抑制効果が立証され、現在では急性増悪期に副腎皮質ステロイド短期間大量静脈内投与を行い、回復期に IFN β の継続的皮内・筋肉内投与を行う方法が、最も一般的な治療法として選択されている。しかし IFN β が全く効果を示さない症例も多い^{2,3)}。すなわち MS は均一な疾患ではなく多様な病態 (phenotypic heterogeneity) を呈する疾患群である可能性が高い。実際 MS は臨床経過から再発寛解型 (relapsing-remitting MS; RRMS), 2 次進行型 (secondary-progressive MS; SPMS), 1 次進行型 (primary-progressive MS; PPMS), 病巣分布から脳型 (conventional MS; CMS) と視神経脊髄型 (opticospinal MS; OSMS),

1) 国立精神・神経センター神経研究所免疫研究部

2) 明治薬科大学薬学部生命創薬科学科生命情報解析学

Department of Immunology, National Institute of Neuroscience, NCNP

Department of Bioinformatics and Neuroinformatics, Meiji Pharmaceutical University

IFN β 治療反応性から responder (RMS), nonresponder (NRMS) に分類される。病理学的にも T 細胞浸潤, 抗体沈着, oligodendrocyte apoptosis の観点から 4 型に分類される⁴⁾。近年 MS の免疫病態の多様性を解析する手法として遺伝子アレイが用いられている。ヒトゲノムプロジェクトの完結によりヒト全遺伝子の塩基配列が解明された結果、遺伝子アレイを用いて個々の細胞における数万遺伝子（ヒト全遺伝子約 30,000）の発現情報を包括的・網羅的・系統的に解析可能になった。RNA 発現解析を transcriptome 解析, タンパク質発現解析を proteome 解析と呼ぶ。網羅的発現解析 (global expression analysis) により、従来の少数分子に焦点を向けた研究 (pinpoint study) では予期しなかった遺伝子群の MS 発症機序における役割が次々明らかになった⁵⁾。また治療による遺伝子発現変化を経時的に解析することにより薬物反応性遺伝子を同定し (薬理ゲノミクス pharmacogenomics), 有効性や副作用を治療開始前に予知することにより、テラーメイド医療 (personalized medicine) に道が開かれた。本稿では DNA マイクロアレイ解析の基本原理と MS の免疫病態解析における応用に関して最近の知見を概説する。

1. DNA マイクロアレイ解析の基本原理

遺伝子アレイはスライドグラスやナイロン膜などの基盤上に、機能既知または未知の数千・万の cDNA または oligonucleotide が貼付けてあるチップである。主として

cDNA をスポットで基盤上にスポットしてある DNA マイクロアレイ (DNA microarray) と光オリゴヌクレオチド合成により基盤上で直接高密度の oligonucleotide を伸長合成している GeneChip (Affymetrix) に分類される (表 1)⁶⁾。スライドグラスを DNA microarray, ナイロン膜を DNA macroarray と総称することもある。最近では約 3,000 種類のタンパク質をスライドグラスに固定してあるプロテインチップ (protein microarray) も普及しており、タンパク質間相互作用 (interactome) やシグナル伝達系の網羅的解析に用いられている⁷⁾。遺伝子アレイは遺伝子多型・変異解析にも応用可能であるが本稿では割愛する。

遺伝子アレイ解析ではまず遺伝子発現レベルの異なる 2 種類以上の細胞・組織、例えば IFN β 投与前後の細胞などから mRNA を抽出し増幅する (図 1)。DNA マイクロアレイでは一般的に別々の蛍光色素 (Cy3, Cy5) でラベルした cDNA または cRNA を作成して同一チップ上で競合的ハイブリダイゼーションを行い、2 色法と呼ばれる。GeneChip では in vitro transcription (IVT) により cDNA から biotin 標識 cRNA を作成、fragment に切断してハイブリダイゼーションを行い、streptoavidin-phycoerythrin (SAPE) を添加して蛍光標識する。GeneChip では 1 サンプルに 1 枚のアレイが必要で、アレイ間の比較になる。どちらの場合もスキャナーで蛍光シグナルを検出し、得られたデータ (dataset) を正規化 (normalization) して統計学的検定を行い、サンプル間の遺伝子発現プロフィール (gene expression profile) を比較解析する。同

表 1 cDNA microarray と GeneChip の比較

	cDNA/Oligonucleotide Microarray	GeneChip
基盤	スライドグラス (microarray) またはナイロン膜 (macroarray)	半導体チップ
固定化法	スポットティングまたは化学合成	オンチップフォトリソグラフ合成
遺伝子	300–1000 bp cDNA or 30–80 mer oligonucleotide	25 mer oligonucleotides of perfect match (PM) and mismatch (MM)
集積度	40,000/slides 程度	>500,000/chip
Tm	不均一	一定
蛍光標識	2 色法 (Cy3, Cy5)	単色法
定量原理	競合的ハイブリダイゼーションによる比較	個々のチップのデーターを正規化して比較
代表的なヒト遺伝子発現解析用アレイ (遺伝子数 ; Commercial Supplier)	Whole Human Genome G4112A Array (41,000; Agilent), Human Whole Genome Bioarray (55,000; Amersham)	Human Genome U133 Plus 2.0 Array (47,000; Affymetrix)
カスタム性	高い 汎用マイクロアレイスキャナーが使用可能	低い 専用のハイブリダイゼーションオーブンや洗浄装置とスキャナーが必要

文献 6 より引用改変。

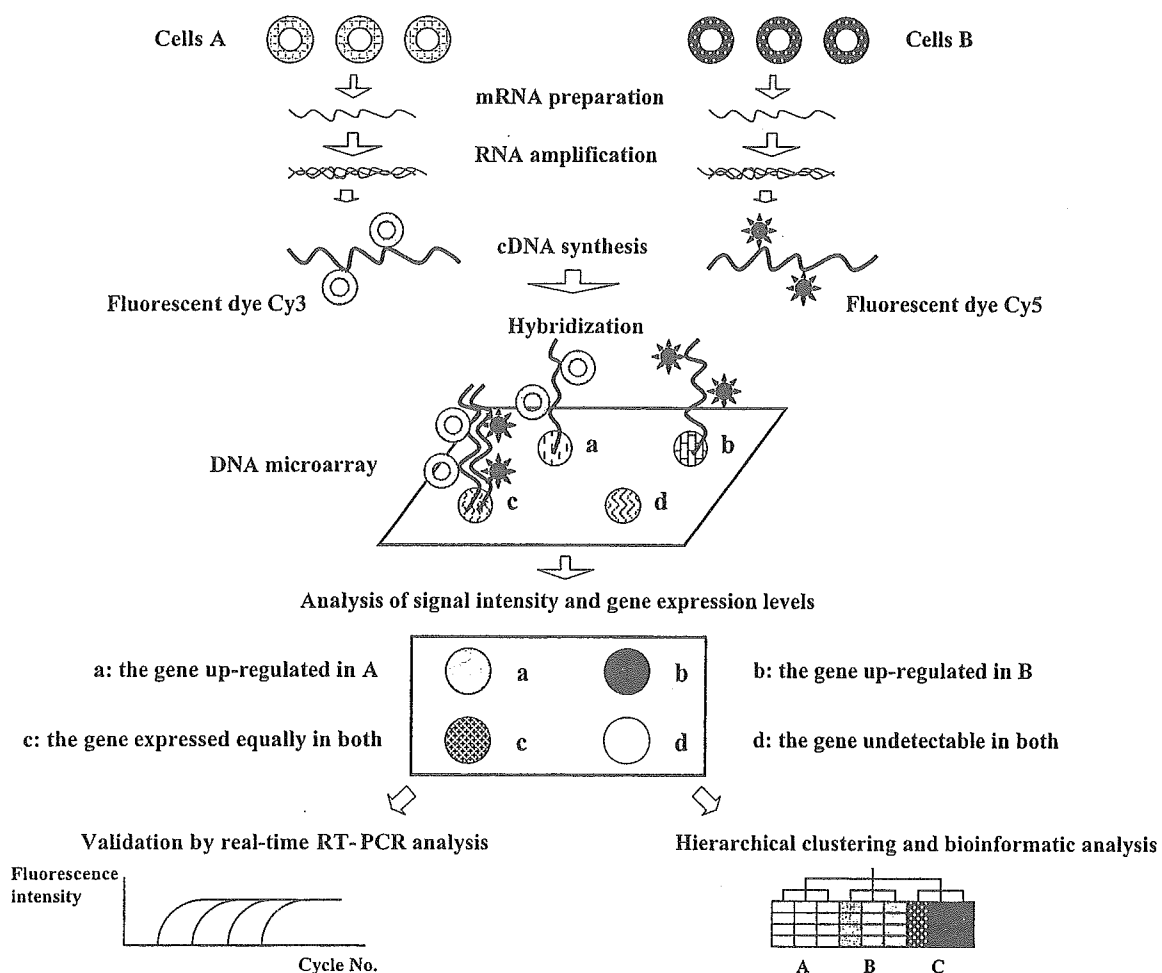


図 1 DNA マイクロアレイ解析の概要。

2種類の細胞から mRNA を抽出増幅し、別々の蛍光色素 (Cy3, Cy5) でラベルした cDNA probe を作成して、cDNA がスポットされたチップ上で競合的ハイブリダイゼーションを行う。スキャナーで蛍光シグナルを検出し、データを正規化して統計学的検定を行い、サンプル間の遺伝子発現プロフィール (gene expression profile) を比較解析する。さらに階層的クラスター解析 (hierarchical clustering analysis) を行って、類似した発現パターンを呈する遺伝子やサンプルをグループに分類する。有意な発現差異を呈する遺伝子は real-time RT-PCR で mRNA を定量して検証する。

定した遺伝子の機能・構造の注釈情報 (annotation) は遺伝子リストの ID から Web 上で database を検索可能である (表 2)。既に様々な細胞・組織の遺伝子発現データが Gene Expression Omnibus (GEO; www.ncbi.nlm.nih.gov/geo) に登録されているが、実験に用いたチップの format が異なるとデータ間の互換性がなくなると考えられ、大規模な meta-analysis を実施する場合に支障となる⁸⁾。サンプル数が多い場合はデータセットの要素の特性を抽出するため、階層的クラスター解析 (hierarchical clustering analysis) を行う⁹⁾。すなわちサンプルに関する事前情報なしに (教師なし法 unsupervised method)、類似した発

現パターンを呈する遺伝子やサンプルをグループに分類して、樹状図 (dendrogram) と発現レベルの 2 次元マトリックスで表示する。またサンプルをいくつかのグループに分類する代表な遺伝子 (discriminator genes) を抽出し、これらを 3 次元に圧縮投射する主成分分析 (principal component analysis) を行う⁹⁾。

我々は薬物応答遺伝子アレイ 1,258 cDNA microarray (Hitachi Life Science) を用いて、MS 患者末梢血 T 細胞の遺伝子発現プロフィールを解析している。健常者 3 名の RNA mixture を universal reference として Cy3 で標識し、患者や健常者のサンプルを全て Cy5 で標識し、各サ

表 2 Transcriptome・proteome 解析に有用な database

Name	Website	Contents
★統合 Database 検索システム		
Entrez	www.ncbi.nlm.nih.gov/Entrez/index.html	The Life Sciences Search Engine
Gene	www.ncbi.nlm.nih.gov/entrez/query.fcgi?CMD=search&DB=gene	A Searchable Database of Genes
OMIM	www.ncbi.nlm.nih.gov/entrez/query.fcgi?CMD=search&DB=omim	Online Mendelian Inheritance in Man
DBGET	www.genome.ad.jp/dbget/dbget.links.html	Web of Molecular Biology Databases
KEGG	www.genome.ad.jp/kegg	Kyoto Encyclopedia of Genes and Genomes
SRS	srs6.ebi.ac.uk	European Bioinformatics Institute Database
HGMD	www.hgmd.cf.ac.uk/hgmd0.html	Human Gene Mutation Database
★配列解析		
UniProt	www.genome.jp/dbget-bin/www_bfind?uniprot	SWISS-PROT Protein Sequence Database
PIR	www.genome.jp/dbget-bin/www_bfind?pir	PIR Protein Sequence Database
BLAST	blast.genome.jp	Sequence Similarity Search
dbSNP	www.ncbi.nlm.nih.gov/entrez/query.fcgi?CMD=search&DB=snp	Single Nucleotide Polymorphism Database
CLUSTALW	align.genome.jp	Multiple Sequence Alignment
TraceSuite II	www-cryst.bioc.cam.ac.uk/~jiye/evoltrace/evoltrace.html	Evolutionary Trace Server
ORF Finder	www.ncbi.nlm.nih.gov/gorf/gorf.html	Open Reading Frame Finder
PROSCAN	thr.cit.nih.gov/molbio/proscan	Web Promoter Scan
★タンパク質立体構造解析		
PDB	www.rcsb.org/pdb	The RCSB Protein Data Bank
RasMol	www.rcsb.org/pdb/help-graphics.html#rasmol_download	Molecular Graphics
GRASS	honiglab.cpmc.columbia.edu/cgi-bin/GRASS/surfserv_enter.cgi	Graphical Representation and Analysis of Structure Server
SWISS-MODEL	swissmodel.expasy.org/SWISS-MODEL.html	An Automated Comparative Protein Modelling Server
ERRAT	nihserver.mbi.ucla.edu/ERRAT	A Protein Structure Verification Algorithm
Verify3D	nihserver.mbi.ucla.edu/Verify_3D	A Crystal Structure Evaluation Server
SCOP	scop.mrc-lmb.cam.ac.uk/scop/index.html	Structural Classification of Proteins
DBAli	salilab.org/DBAli	A Database of Structure Alignments
★タンパク質機能予測		
SOSUI	sosui.proteome.bio.tuat.ac.jp/sosuiframe0.html	Classification and Secondary Structure Prediction of Membrane Proteins
PSORT II	psort.ims.u-tokyo.ac.jp	Prediction of Protein Sorting Signals and Localization Sites in Amino Acid Sequences
SignalP 3.0	www.cbs.dtu.dk/services/SignalP	Prediction of Signal Peptide Cleavage Sites in Amino Acid Sequences
InterPro	www.ebi.ac.uk/interpro	A Database of Protein Families, Domains and Functional Sites
PredictProtein	www.embl-heidelberg.de/predictprotein/predictprotein.html	Structure Prediction and Sequence Analysis
BIND	www.bind.ca	The Biomolecular Interaction Network
DIP	dip.doe-mbi.ucla.edu	Databases of Interacting Proteins
MINT	160.80.34.4/mint/index.php	A Molecular Interaction Database
PPID	www.anc.ed.ac.uk/mscs/PPID/cgi-bin/ppid_search.pl	Protein-Protein Interaction Database
PROCAT	www.biochem.ucl.ac.uk/bsm/PROCAT/PROCAT.html	A Database of 3D Enzyme Active Site Templates
Scansite	scansite.mit.edu	A Motif Scan
PhosphoSite	www.phosphosite.org/Login.jsp	An In Vivo Phosphorylation Site Database
ExPASy	au.expasy.org	Expert Protein Analysis System Proteomics Server

2005年8月の時点でのサイト。

ンプルで遺伝子ごとに Cy5/Cy3 signal intensity ratio を測定している。比較する 2 群間 (MS vs 健常者など) で有意な発現差異を呈する遺伝子は、Bayesian t test または R

解析 (www.cran.r-project.org) と Bonferroni 補正で統計学的有意性を検定することにより同定している。さらに有意な遺伝子に関しては、LightCycler (Roche) による

real-time RT-PCRで定量してアレイ解析の結果を検証(validation)している。階層クラスター解析と主成分解析は GeneSpring (Silicon Genetics-Agilent) で行っている。末梢血リンパ球の遺伝子アレイ解析の問題点は、特定の遺伝子の発現レベルが年齢・性・喫煙・飲酒・常用薬・嗜好品・精神的ストレスなどの個人差や採血時刻(日内変動)の影響を受けることである(interindividual and intraindividual variation)¹⁰。また脳組織の遺伝子アレイ解析の問題点は死後脳凍結までに要する時間(RNA degradation time)で、組織のpHがある程度参考になる。

2. DNAマイクロアレイによる多発性硬化症の免疫病態の解析

2.1. MS脳組織の網羅的遺伝子発現解析

DNAマイクロアレイによるMSの病態解析の最初の報告はWhitneyらによる研究である¹¹。彼らは独自のcDNA microarrayを用いてMS急性期炎症性病巣と正常白質(normal-appearing white matter; NAWM)を比較し、MS病巣におけるinterferon-regulatory factor IRF-2, 5-lipoxygenase発現上昇を報告した(表3)^{11,12}。ChabasらはMS brain cDNAライブラリーの網羅的シークエンス解析でosteopontin(OPN)発現レベルの上昇を認めた¹³。さらにラットEAE脊髄のカスタム oligonucleotide microarray解析でOPNの発現上昇を確認した。OPNは主としてT細胞が産生しmacrophagesによるIL-12産生を促進してIL-10産生を抑制するTh1 cytokineで、活動性RRMS患者血清で上昇している¹⁴。OPN遺伝子欠損マウスはEAE惹起に対して抵抗性を示す¹³。LockらはGeneChipを用いてMS急性炎症性病巣と慢性非活動性病巣を比較し、活動性病巣でのgranulocyte colony stimulating factor(G-CSF)発現上昇と非活動性病巣でのIgG Fc receptor, IgE receptor, histamine receptor type 1の発現上昇を認めた¹⁵。さらに彼らはG-CSF投与でEAEを軽症化出来ること、immunoglobulin FcR γ-chain遺伝子欠損マウスではEAE慢性化が抑制されることを証明し、アレイ解析の結果を裏付けた。ChabasらやLockらの報告により、MS, EAEの病巣形成におけるallergic response mediatorsの役割が認識されるようになった¹⁶。

MyckoらはcDNA microarray(Clontech)を用いてSPMSの慢性活動性病巣と非活動性病巣、脱髓鞘辺縁部と中心部を比較し、活動性病巣辺縁部における炎症・免疫応答遺伝子群(TNFαなど)の発現上昇を認めた¹⁷。Graumann

らはcDNA macroarray(Clontech)を用いてMSのNAWMと非神経疾患のコントロール白質を比較し、NAWMにおける脳虚血関連遺伝子(hypoxia-inducible factor 1 alpha; HIF-1αなど)の発現上昇を認めた¹⁸。LindbergらはGeneChipでSPMSの活動性病巣とNAWMを比較し、活動性病巣でのimmunoglobulin産生亢進の所見を見出した¹⁹。Tajouriらは独自のcDNA microarrayを用いてSPMSの急性・慢性活動性病巣をnon-MSコントロール白質と比較し、活動性病巣におけるα-B-crystallin, superoxide dismutase SOD1の発現上昇を報告した²⁰。上述のMS脳組織のマイクロアレイ解析は各々症例数が少なく、RNA抽出部位が必ずしも全体像を反映していない可能性は否定出来ない。EAE脳・脊髄の網羅的遺伝子発現解析に関しては割愛する²¹⁻²³。

2.2. 末梢血リンパ球を用いたMSと健常コントロールの比較解析

RamanathanらはResearch Genetics(Invitrogen)のGene-Filter membrane arrayを用いて、MSと健常者のmonocyte-depleted peripheral blood lymphocytes(PBL)を比較し、MSにおけるlymphocyte-specific protein tyrosine kinase(LCK), IL-7Rの発現上昇を報告した²⁴。LCKはAirlaらによるRRMSのPBMCのcDNA macroarray(Clontech)解析で、intravenous methylprednisolone pulse(IVMP)で発現低下する遺伝子として報告されている²⁵。Bomprezziらは独自のcDNA microarrayを用いて、24例のRRMSと21名の健常者のperipheral blood mononuclear cells(PBMC)を比較し、発現差異を示した53遺伝子を同定した²⁶。MSでは自己反応性T細胞活性化に関連するIL-7R, ZAP70, TNFRSF7(CD27)の発現上昇およびサイトカインmRNAのubiquitin-proteasome系による分解を制御するHSPA1A(HSP70)の発現低下を認めた。MayneらはRRMSと健常者のCD4陽性T細胞をnegative selectionで分離し、cDNA membrane array(NIA)を用いて解析し、MSにおけるcytoplasmic FMR1 interacting protein 2(CYFIP2)の発現上昇を認めた²⁷。

我々はcDNA microarray(Hitachi Life Science)を用いて、72例のMS(65 RRMS, 7 SPMS)と22名の健常者の末梢血CD3陽性T細胞、CD3陰性non-T細胞の遺伝子発現プロフィールを解析した(表3)²⁸。その結果T細胞で173遺伝子、non-T細胞で50遺伝子の発現差異を認め、上位30遺伝子(the most significant genes)を抽出すると、T細胞で25遺伝子(NR4A2, TCF8)の上昇と

表 3 Microarray による MS の免疫病態の解析

Authors (Reference No.)	Year	No of MS Patients and Controls	RNA Samples
Whitney et al. (11)	1999	PPMS (n=1)	acute lesion vs NAWM
Ramanathan et al. (24)	2001	RRMS (n=15) vs HC (n=15)	monocyte-depleted PBL
Wandinger et al. (35)	2001	RRMS (n=1) plus HC (n=2)	PBMC incubated with IFN β in vitro
Whitney et al. (12)	2001	PPMS (n=1), RRMS (n=1), EAE vs HC (n=3)	acute or chronic lesions of MS and EAE vs white matter of non-MS controls
Lock et al. (15)	2002	CPMS and SPMS (n=4)	acute or chronic active lesions vs chronic silent lesions
Mass et al. (32)	2002	RA (n=20), SLE (n=24), IDDM (n=5), and MS (n=5) vs HC before and after influenza vaccination (n=9)	PBMC
Bomprezzi et al. (26)	2003	RRMS (n=18), SPMS (n=6) vs HC (n=21)	PBMC (fresh or frozen)
Graumann et al. (18)	2003	SP/PP/RRMS (n=10) vs non-neurological controls (n=7)	NAWM vs control white matter
Koike et al. (36)	2003	RRMS (n=13) before and at 3 and 6 months after IFN β treatment	T and non-T cells separated from PBMC
Mycko et al. (17)	2003	SPMS (n=4)	chronic active vs silent lesions and the lesion margin vs center
Stürzebecher et al. (46)	2003	RRMS before and after IFN β treatment for 6 months (n=10; 6 responders vs 4 non-responders)	frozen PBMC ex vivo or incubated with IFN β in vitro
Tajouri et al. (20)	2003	SPMS (n=5) vs non-MS	acute and chronic active lesions
Weinstock-Guttman et al. (44)	2003	RRMS before and at 1, 2, 4, 8, 24, 120, and 160 h after IFN β treatment (n=8)	monocyte-depleted PBL
Achiron et al. (29)	2004	RRMS (n=26; 14 with treatment) vs HC (n=18)	PBMC
Achiron et al. (30)	2004	RRMS treated (n=13) vs untreated (n=13)	PBMC
Airla et al. (25)	2004	RRMS (n=6) before and after IVMP	PBMC
Hong et al. (47)	2004	RRMS/SPMS treated with IFN β (n=18), GA (n=12) or untreated (n=15)	PBMC
Iglesias et al. (33)	2004	RRMS (n=17) vs HC (n=7)	PBMC
Lindberg et al. (19)	2004	SPMS (n=6) vs non-neurological controls (n=12)	active lesions vs NAWM
Mandel et al. (31)	2004	RRMS (n=13) vs SLE (n=5) vs HC (n=18)	PBMC
Mayne et al. (27)	2004	RRMS (n=21) vs HC (n=19)	CD4 $^+$ T cells
Satoh et al. (28)	2005	RRMS (n=65) plus SPMS (n=7) vs HC (n=22)	T and non-T cells separated from PBMC

Abbreviations: RRMS, relapsing-remitting MS; SPMS, secondary progressive MS; PPMS, primary progressive MS; CPMS, chronic progressive MS; HC, healthy controls; IDDM, insulin-dependent diabetes mellitus; NAWM, normal appearing white matter; PBMC, peripheral blood mononuclear cells; PBL, peripheral blood lymphocytes; IFN, interferon; GA, glatiramer acetate; IVMP, intravenous methylprednisolone pulse.

MAPK1, SMARCA3, HSPA1A, TRAIL, TOP1, CCR5, BAG1, DAXX, TSC22, PARP の低下など), non-T 細胞で 27 遺伝子 (ICAM1, CDC42, RIPK2, SODD, TOP2A の上昇と BCL2, RPA1, NFATC3, HSPA1L, RBBP4, PRKDC の低下など) が apoptosis 制御遺伝子に属していた。すなわち apoptosis 促進遺伝子 (proapoptotic genes)

と抑制遺伝子 (antiapoptotic genes) の発現上昇・低下の拮抗的バランス (counterbalance) を認め, MS 免疫病態における apoptosis 制御機構の異常が示唆された。Achiron らは GeneChip を用いて、26 例の RRMS と 18 名の健常者の PBMC を比較解析した²⁹⁾。両群間で 1,109 遺伝子の発現差異を認め、MS における T 細胞活性化関連遺伝子

Type of Microarray	No of Genes on Microarray	Key Findings
Original cDNA Glass Array	1,344 or 5,000	Upregulation of IRF-2 and TNFRp75 in acute lesions
GeneFilters GF211 Membrane Array (Research Genetics)	5,184	Upregulation of LCK, IL-7R and MMP-19 and downregulation of CCR6 and DFFA in MS
Mini-Lymphochip cDNA Array	6,432	Upregulation of proinflammatory genes such as CCR5, IP-10, and IL-15RA by IFN β treatment
Original cDNA Glass Array	2,798	Upregulation of 5-lipoxygenase in MS and EAE lesions
HuGene FL Oligonucleotide Array (Affymetrix)	7,026	Upregulation of G-CSF in active lesions and upregulation of IgG FcR in silent lesions, and amelioration of EAE in FcR γ -chain-KO mice and by treatment with G-CSF
GeneFilters GF211 Membrane Array (Research Genetics)	4,329	Indistinguishable profiles between MS and IDDM and downregulation of apoptosis-regulatory genes in autoimmune diseases
Original cDNA Array (Modified Lymphochip)	6,500 or 7,500	Upregulation of PAFAH1B1, IL-7R, ZAP70, and TNFRSF7(CD27) and downregulation of HSPA1A (HSP70) and CKS2 in MS
Atlas Human cDNA Membrane Array 1.2 (Clontech)	3,528	Upregulation of ischemic preconditioning genes such as HIF-1 α in NAWM of MS
Human cDNA Array (Hitachi Life Science)	1,258	Upregulation of 15 IFN-responsive genes in MS after IFN β treatment
Atlas Human 1.0 Glass Microarray (Clontech)	588	Upregulation of inflammation/immune-related genes in the margin of active lesions
Mini-Lymphochip cDNA Array	6,432 or 12,672	Downregulation of IL-8 in responders after IFN β treatment
Custom-made cDNA Glass Array	5,000	Upregulation of α B-crystallin and SOD in acute lesions
GeneFilters GF211 Membrane Array (Research Genetics)	5,184	Time-dependent upregulation of IFN-responsive genes
Human U95Av2 Oligonucleotide Array (Affymetrix)	12,000	Upregulation of T cell activation genes and downregulation of IL-1 and TNF signaling genes in MS
Human U95Av2 Oligonucleotide Array (Affymetrix)	12,000	Identification of SCYA4, IL2RG, and TNFRSF6(Fas) as immunomodulatory treatment-associated genes
Atlas Human Hematology/Immunology Membrane Array (Clontech)	448	Downregulation of LCK, TCF7, CD5, and ISGF3 by IVMP
Original Membrane Array	36	Distinct gene expression profile between MS patients treated with IFN β and GA
HuGene FL Oligonucleotide Array (Affymetrix)	6,800	Upregulation of E2F transcription factor pathway genes in MS
Human U95A Oligonucleotide Array (Affymetrix)	12,633	Upregulation of genes related to Ig synthesis in active lesions of MS
Human U95Av2 Oligonucleotide Array (Affymetrix)	12,000	Downregulation of NR4A1 and NR4A3 as the autoimmunity-specific signature
Immune Membrane Array (National Institute on Aging)	1,152	Upregulation of CYFIP2 in MS
Human cDNA Array (Hitachi Life Science)	1,258	Aberrant expression of apoptosis and DNA damage-regulatory genes in MS

(LEF1, TCF3, SLAM, ITGB2, CTSB) の発現上昇および IL-1 β , TNF α シグナル伝達系遺伝子の発現低下を認めた。我々の結果²⁸⁾に反し、MS における orphan nuclear receptor NR4A2 の発現低下を報告した。彼らの研究では MS 14 例は採血時に IFN β , glatiramer acetate (GA), IVIg 治療中である点が問題である。彼らは同じ症例の治療中

13 例と未治療 13 例の PBMC の比較解析を行い、治療関連 7 遺伝子 (TNFRSF6; Fas など) を同定した³⁰⁾。さらに 13 例の RRMS と 5 例の SLE を 18 名の健常者と比較して、自己免疫疾患共通遺伝子 (autoimmunity-specific signature) を探索し、自己免疫疾患における apoptosis, matrix metalloproteinase (MMP) 制御系遺伝子の発現異

常を発見した³¹⁾。Maas らも 20 例の RA, 24 例の SLE, 5 例の IDDM, 5 例の MS と 9 名の健常者 (influenza ワクチン接種前後) の PBMC を比較解析した³²⁾。ワクチンに対する免疫応答と自己免疫疾患の遺伝子発現プロファイルは全く異なるが、RA と SLE, MS と IDDM は極めて類似し、自己免疫疾患では共通して apoptosis 制御遺伝子群の発現低下を認めることを報告した。Iglesias らは GeneChip を用いて 17 例の RRMS と 10 名の健常者の PBMC を比較し、MS における E2F transcription factor pathway 遗伝子群の発現上昇を見出し、E2F1 遺伝子欠損マウスでは EAE が軽症化することを報告した³³⁾。

2.3. MS におけるインターフェロンベータ治療反応性の解析

我々は cDNA macroarray (Invitrogen) を用いて、ヒト胎児脳より樹立したアストロサイト (astrocytes) 純培養で IFN β , IFN γ により発現変動する遺伝子群を解析した³⁴⁾。IFN β による interferon-regulatory factor IRF-7 と pleiotrophin の発現上昇, IFN γ による IRF-1 と ICAM-1 の発現上昇を発見した。Wandinger らは RRMS と健常者の PBMC を IFN β で刺激して cDNA microarray (Mini-Lymphochip) を用いて解析した³⁵⁾。彼らは proinflammatory molecules である CC chemokine receptor 5 (CCR5), interferon-inducible cytokine IP-10 (CXCL10), IL15 receptor alpha (IL-15RA) の発現上昇を認めた。我々は cDNA microarray (Hitachi Life Science) を用いて、13 例の RRMS の末梢血 CD3 陽性 T 細胞と CD3 隆性 non-T 細胞で、IFN β 1b 治療開始後に発現変動したインターフェロン応答遺伝子群 (IFN-responsive genes; IRG) を同定した³⁶⁾。21 遺伝子が有意な変動を呈し、T 細胞で 8 IRG (IRF-7, ISG15, IFI56, IFI6-16, IFI60, IFI30, ATF3, TLR5) の発現上昇, IL-3, monokine induced by IFN γ (MIG) などの発現低下を認め、non-T 細胞では 12 IRG (IRF-7, ISG15, IFI56, IFI6-16, IFI27, IFI17, TAP1, TNFAIP6, TSC22, SULT1C1, RPC39, RAB11A) の発現上昇, IL-3 の発現低下を認めた。ISG15, IFI56, IFI6-16, IFI27, TSC22, SULT1C1 に関しては、治療開始後 3-6 ヶ月の持続的な上昇を認めた。一方統計学的有意差は見られなかつたが、治療後に Th1 関連遺伝子 CCR5 (T), IFN γ (T), TNF α (non-T) の発現上昇傾向を認めた。このことは MS において IFN β 治療は必ずしも明確な Th2 shift を誘導しないという見解³⁵⁾に一致する。上記のうち 9 遺伝子 (IRF7, ISG15, IFI56, IFI6-16, IFI60, IFI17, TAP1, TNFAIP6,

MIG) はプロモーター領域に IFN-stimulated response element (ISRE) や IRF element (IRF-E) が同定されている既知の IRG であり、IFN β 治療に直接反応して上昇し治療効果発現に深く関与していると考えられる。興味深いことに培養系では多くの IRG は IFN γ によっても発現が誘導される^{36,37)}。IRF-7 はウイルス感染時に IFN α/β 産生を増幅する正の制御因子である³⁸⁾。IFI30 は class II MHC 拘束性抗原提示に働くチオール還元酵素であり、IFI30 遺伝子欠損マウスでは抗原呈示能低下を来す³⁹⁾。TAP1 は class I MHC 拘束性抗原提示を司るペプチド輸送因子で、TAP1 遺伝子欠損マウスでは CD8+ T 細胞を介する結核菌への抵抗力が減弱する⁴⁰⁾。TNFAIP6 は TNF α , IL-1 β により発現誘導される分泌蛋白質で、マウス関節炎に投与すると抗炎症作用を呈する⁴¹⁾。以上より MS において IFN β は antiviral and antiinflammatory mediator 遺伝子群の発現上昇を誘導することが明らかになった。非常に興味深いことに SLE では治療に関わらず PBMC における IRG の発現レベルが高い^{42,43)}。

Weinstock-Guttmann らは GeneFilter membrane array を用いて、8 例の RRMS で IFN β 1a 投与後経時的に monocyte-depleted PBL を解析して IRG を同定したが、その多くは我々の結果とオーバーラップしている⁴⁴⁾。また Liang らは Weinstock-Guttmann らのデータを再解析し、IFN β により発現誘導される IRG は early-onset (within 8 hours), intermediate-onset (24 hours), late-onset (48 hours) の 3 群に分類されることを報告した⁴⁵⁾。Stürzebecher らは cDNA microarray (Mini-Lymphochip) を用いて、10 例の RRMS で IFN β 1b 治療前後の PBMC を解析した⁴⁶⁾。治療開始前 6 ヶ月から開始 12 ヶ月後まで毎月 Gd 造影 MRI で活動性病巣数を算出し、治療後に病巣数が 60% 以上減少した症例を responder と定義した。また nonresponder を治療開始後から効果のない nonresponder from initiation of therapy (INR) と、治療開始後一定期間は効果があり neutralizing antibody (NAb) 出現とともに効果が減弱した nonresponder with development of NAb (NAbNR) の 2 群に分類した。さらに ex vivo 解析と同時に IFN β で刺激した in vitro 解析も行った。Responder で治療後 2 倍以上変動した遺伝子は ex vivo では 25 遺伝子 (IFI17, OAS, Stat1 の上昇と IL-8, CD69, c-fos, TSC22 の低下など) で、そのうち IL-8 発現低下は responder の指標となる可能性が示唆された。一方 in vitro IRG は 87 遺伝子で、responder と nonresponder の間で発現レベルに差異を認めなかっ

た。彼らの結果に反して、我々は IFN β 治療後に non-T 細胞で TGF β -stimulated protein TSC22 の発現上昇を認めている³⁶。彼らの研究の問題点は responder 6 例・INR 2 例・NAbNR 2 例と症例数が少なく、PBMC を凍結保存後に解凍して刺激しており、実験操作で遺伝子発現が変化し得ることである⁴⁶。さらに 1 例の responder では治療前に約 90 個の Gd 造影病巣を呈しているが、これほど多数の造影病巣を示す症例は日本人 MS では極めて異例である。Hong らは免疫応答に極めて重要な 36 遺伝子に絞った cDNA macroarray を作成し、未治療 MS と IFN β 1a または GA 治療症例の PBMC を解析し、治療反応性遺伝子群の相違を明らかにした⁴⁷。興味深いことに活性化 T 細胞の血液脳関門通過に重要な MMP-9 の発現は IFN β により低下したが GA では上昇した。

van Boxel-Dezire らは 26 例の IFN β 1b 治療中の RRMS で PBMC のサイトカイン遺伝子発現レベルを半定量的 RT-PCR で経時的に解析した⁴⁸。治療前後 2 年間の再発回数・IVMP 回数・Extended Disability Status Scale (EDSS) スコアから 16 例の responder と 10 例の nonresponder に分けて比較すると、responder は治療前に IL-12p35 発現レベルが低い傾向を呈した。Wandinger らは RRMS で IFN β 1a 治療後 1 年間一度も再発がなく、EDSS スコア悪化の見られない症例を responder、一度以上再発が見られた症例を nonresponder と定義し、20 例の responder と 19 例の nonresponder の PBMC を比較し、responder では TNF-related apoptosis-inducing ligand (TRAIL; TNFSF10) が持続的高値を呈することを報告した⁴⁹。TRAIL は IRG の 1 つで我々は MS の T 細胞における発現低下を認めている²⁸。TRAIL 遺伝子欠損マウスは胸腺細胞の apoptosis に異常を来たし、コラーゲン関節炎などに高感受性になることが報告されている⁵⁰。Baranzini らは 52 例の IFN β 治療中の RRMS で経時的に PBMC の 70 遺伝子の発現レベルを RT-PCR で定量的に解析した。彼らは治療後 2 年間一度も再発がなく、EDSS スコア悪化の見られない症例を responder、2 回以上再発が見られた症例を nonresponder と定義し、両者は 3 遺伝子 (caspase2, caspase10, FLICE inhibitory protein; FLIP) の発現レベルの 3 次元解析で 86% 区別可能と報告している⁵¹。

最近我々は前述²⁸の 72 例の IFN β 未治療 MS (46 例は初回採血後 2 年間 IFN β 治療開始) と 22 名の健常者の末梢血 CD3 陽性 T 細胞を cDNA microarray (Hitachi Life Science) を用いて解析したデータを、両群間で発現差異

を示す 286 遺伝子を指標にして階層的クラスター解析で再解析した (Satoh et al. Manuscript in preparation)。この解析により 286 遺伝子は class #1-#5 に分類され、MS は健常者から分離されてさらに 4 つのサブグループに分類された。すなわち遺伝子発現プロフィールが健常者に近似した A 群、治療導入前後 2 年間の再発回数・IVMP 日数・入院日数の点で最も活動性が高い B 群、大脳限局病変が多い C 群、最も EDSS スコアが高値の D 群に分類された。B 群は chemokine 遺伝子を多く含む class #5 の発現レベルが高かった。また IFN β 治療前後 2 年間の再発回数・IVMP 日数・入院日数・EDSS スコア・MRI T2 強調画像病巣数の比較と患者満足度から算出した IFN β 治療反応スコアで評価すると、responder は A 群と B 群に集積していた。また responder では nonresponder に比較して治療開始後 6 ヶ月の時点でも IRG (ISG15, IFI27, MCP-1, TNFRp75) の発現レベルが高く保持される傾向を示した。

3. 結 語

我々は DNA マイクロアレイ解析を用いて MS が T 細胞の遺伝子発現プロフィールに基づき 4 群に分類され、各群は疾患活動性・病変分布・IFN β 治療反応性との対応を認めることを報告した。現在、欧米人 MS にも同様の結果が当てはまるかどうか症例数を増加して解析中である。このような研究成果を積み重ねることにより MS のテラメイド医療樹立に貢献出来るとと思われる。

謝 辞

本稿で紹介した我々研究の一部は、平成 17 年度厚生労働科学研究費補助金こころの健康科学（遺伝子アレイによる多発性硬化症再発予測法樹立に関する研究：H17-こころ-020）および平成 17 年度創薬等ヒューマンサイエンス総合研究事業（DNA マイクロアレイによる多発性硬化症の迅速診断法の樹立に関する研究：KH21101）の補助により実施された。

参考文献

- Sospedra M, Martin R. Immunology of multiple sclerosis. *Annu Rev Immunol* 23: 683–747, 2005.
- Wabant E, Vukusic S, Gignoux L, Dubief FD, Achiti I, Blanc S, Renoux C, Confavreux C. Clinical characteristics of responders to interferon therapy for relapsing MS. *Neurology* 61: 184–189, 2003.

- 3) Rudick RA, Lee J-C, Simon J, Ransohoff RM, Fisher E. Defining interferon β response status in multiple sclerosis patients. *Ann Neurol* 56: 548–555, 2004.
- 4) Lucchinetti C, Brück W, Parisi J, Scheithauer B, Rodriguez M, Lassmann H. Heterogeneity of multiple sclerosis lesions: implications for the pathogenesis of demyelination. *Ann Neurol* 47: 707–717, 2000.
- 5) Steinman L, Zamlil S. Transcriptional analysis of targets in multiple sclerosis. *Nature Rev Immunol* 3: 483–492, 2003.
- 6) 野村 仁. ゲノム創薬. 個別化医療とゲノムデータマイニング. 新・生命科学ライブラリ - バイオと技術 5. 第4章ゲノム創薬各論. サイエンス社. pp. 55–129, 2005.
- 7) Chan SM, Ermann J, Su L, Fathman CD, Utz PJ. Protein microarrays for multiplex analysis of signal transduction pathways. *Nature Med* 10: 1390–1396, 2004.
- 8) Stevens JR, Doerge RW. Combining Affymetrix microarray results. *BMC Bioinformatics* 6: 57–75, 2005.
- 9) 戸塚裕彦. データのコンピュータ解析. データの標準化と解析ソフト. 実験医学別冊 DNA チップ実験まるわかり. 佐々木博巳・青柳一彦編. 羊土社. pp. 80–90, 2004.
- 10) Whitney AR, Diehn M, Popper SJ, Alizadeh AA, Boldrick JC, Relman DA, Brown PO. Individuality and variation in gene expression patterns in human blood. *Proc Natl Acad Sci USA* 100: 1896–1901, 2003.
- 11) Whitney LW, Becker KG, Tresser NJ, Caballero-Ramos CI, Munson PJ, Prabhu VV, Trent JM, McFarland HF, Biddison WE. Analysis of gene expression in multiple sclerosis lesions using cDNA microarrays. *Ann Neurol* 46: 425–428, 1999.
- 12) Whitney LW, Ludwin SK, McFarland HF, Biddison WE. Microarray analysis of gene expression in multiple sclerosis and EAE identifies 5-lipoxygenase as a component of inflammatory lesions. *J Neuroimmunol* 121: 40–48, 2001.
- 13) Chabas D, Baranzini SE, Mitchell D, Bernard CC, Rittling SR, Denhardt DT, Sobel RA, Lock C, Karpuk M, Pedotti R, Heller R, Oksenberg JR, Steinman L. The influence of the proinflammatory cytokine osteopontin on autoimmune demyelinating disease. *Science* 294: 1731–1735, 2001.
- 14) Vogt MH, Lopatinskaya L, Smits M, Polman CH, Nagelkerken L. Elevated osteopontin levels in active relapsing-remitting multiple sclerosis. *Ann Neurol* 53: 819–822, 2003.
- 15) Lock C, Hermans G, Pedotti R, Brendolan A, Schadt E, Garren H, Langer-Gould A, Strober S, Cannella B, Allard J, Klonowski P, Austin A, Lad N, Kaminski N, Galli SJ, Okenberg JR, Raine CS, Heller R, Steinman L. Gene-microarray analysis of multiple sclerosis lesions yields new targets validated in autoimmune encephalomyelitis. *Nature Med* 8: 500–508, 2002.
- 16) Pedotti R, DeVoss JJ, Youssef S, Mitchell D, Wedemeyer J, Madanat R, Garren H, Fontoura P, Tsai M, Galli SJ, Sobel RA, Steinman L. Multiple elements of the allergic arm of the immune response modulate autoimmune demyelination. *Proc Natl Acad Sci USA* 100: 1867–1872, 2003.
- 17) Mycko MP, Papoian R, Boschert U, Raine CS, Selma JW. cDNA microarray analysis in multiple sclerosis lesions: detection of genes associated with disease activity. *Brain* 126: 1048–1057, 2003.
- 18) Graumann U, Reynolds R, Steck AJ, Schaeren-Wiemers N. Molecular changes in normal appearing white matter in multiple sclerosis are characteristic of neuroprotective mechanisms against hypoxic insult. *Brain Pathol* 13: 554–573, 2003.
- 19) Lindberg RLP, De Groot CJA, Certa U, Ravid R, Hoffmann F, Kappos L, Leppert D. Multiple sclerosis as a generalized CNS disease-comparative microarray analysis of normal appearing white matter and lesions in secondary progressive MS. *J Neuroimmunol* 152: 154–167, 2004.
- 20) Tajouri L, Mellick AS, Ashton KJ, Tannenberg AEG, Nagra RM, Tourtellotte WW, Griffiths LR. Quantitative and qualitative changes in gene expression patterns characterize the activity of plaques in multiple sclerosis. *Mol Brain Res* 119: 170–183, 2003.
- 21) Ibrahim SM, Mix E, Böttcher T, Koczan D, Gold R, Rolfs A, Thiesen H-J. Gene expression profiling of the nervous system in murine experimental autoimmune encephalomyelitis. *Brain* 124: 1927–1938, 2001.
- 22) Carmody RJ, Hilliard B, Maguschak K, Chodosh LA, Chen YH. Genomic scale profiling of autoimmune inflammation in the central nervous system: the nervous response to inflammation. *J Neuroimmunol* 133: 95–107, 2002.
- 23) Baranzini SE, Bernard CCA, Oksenberg JR. Modular transcriptional activity characterizes the initiation and progression of autoimmune encephalomyelitis. *J Immunol* 174: 7412–7422, 2005.
- 24) Ramanathan M, Weinstock-Guttman B, Nguyen LT, Badgett D, Miller C, Patrick K, Brownscheidle C, Jacobs L. In vivo gene expression revealed by cDNA arrays: the pattern in relapsing-remitting multiple sclerosis patients compared with normal subjects. *J Neuroimmunol* 116: 213–219, 2001.
- 25) Airila N, Luomala M, Elovaara I, Kettunen E, Knuutila S, Lehtimäki T. Suppression of immune system genes by methylprednisolone in exacerbations of multiple sclerosis. Preliminary results. *J Neurol* 251: 1215–1219, 2004.
- 26) Bompelli R, Ringnér M, Kim S, Bittner ML, Khan J, Chen Y, Elkahloun A, Yu A, Bielekova B, Meltzer PS, Martin R, McFarland HF, Trent JR. Gene expression profile in multiple sclerosis patients and healthy controls: identifying pathways relevant to disease. *Hum Mol Genet* 12: 2191–2199, 2003.
- 27) Mayne M, Moffatt T, Kong H, McLaren PJ, Fowke KR, Becker